Quantum Dots as Immunoassay Probes

Roger M. Leblanc

UNIVERSITY OF Miami

Introduction – quantum dots

Definition

- A material that confines electrons in 3D
- 1-10 nm length scale (for most semiconductors)

CdSe QDs

(2.2, 2.6, 3.2, 4.3, and 5.5 nm)

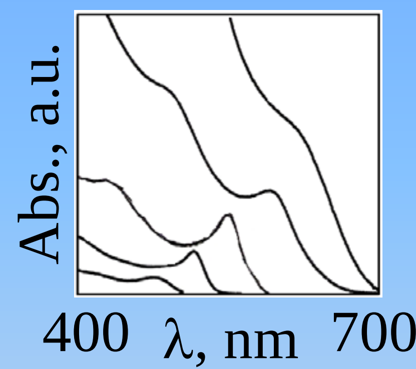

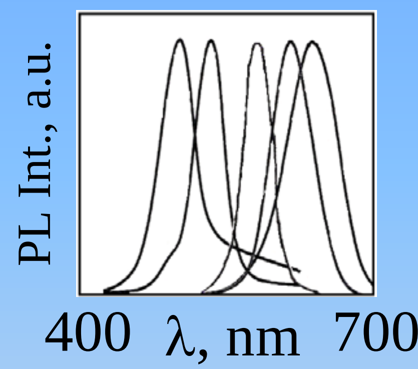

Properties

- Size dependent emission
- Narrow emission band: fwhm 35 nm
- High quantum yields: $\leq$ 85 %
- Broad excitation spectra
- Chemical/photo stability

d = 1.9 2.4 4.1 5.2 nm

λ_{ex} = 365 nm

CdS-Peptide QDs – Cu^{2+} Detection

Peptide

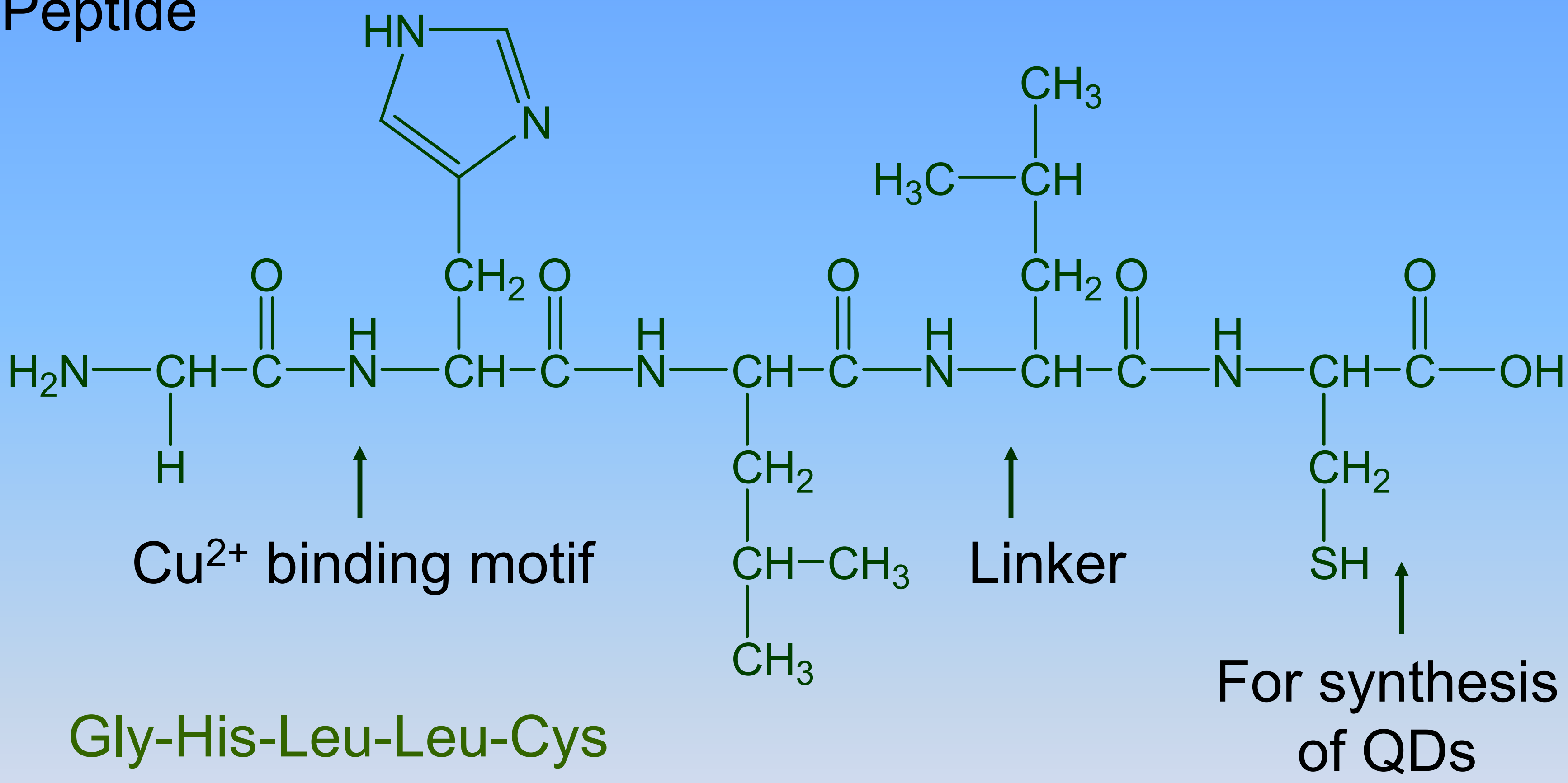

Gly-His-Leu-Leu-Cys

Fmoc solid phase synthesis, MW = 541.67

H_2O soluble, white powder, Yield = 79 %, Purity = 96 %

Gattás-Asfura, K. M. et al. Chem. Commun. 2003, 2684-2685.

CdS-Peptide QDs – Cu^{2+} Detection

Cd^{2+}

↓ Peptide

↓ pH 7.5-8.5, [NaOH]

↓ S^{2-}

[1×10^{-3} M]

Gly-His-Leu-Leu-Cys-CdS

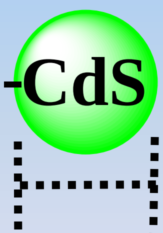

24 Å

Aggregates visible in solution

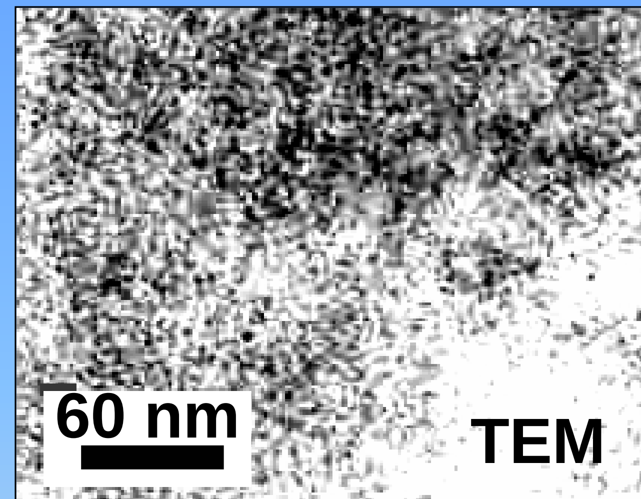

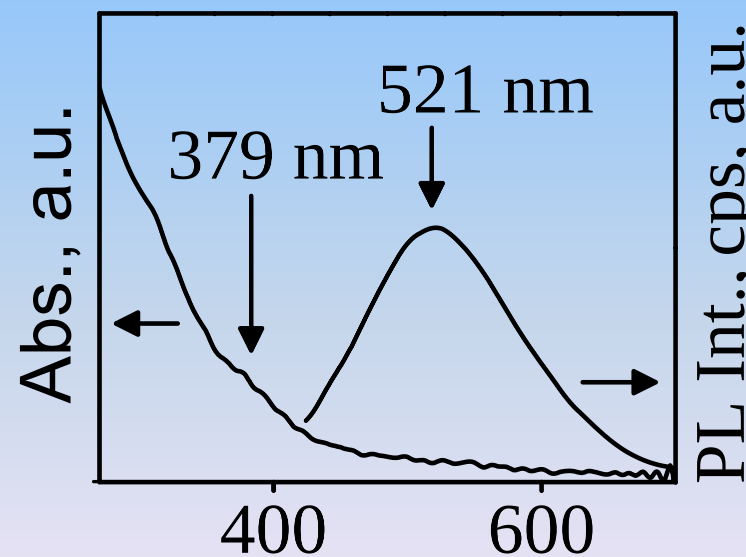

Gattás-Asfura, K. M. et al. Chem. Commun. 2003, 2684-2685.

CdS-Peptide QDs – Cu^{2+} Detection

Selectivity

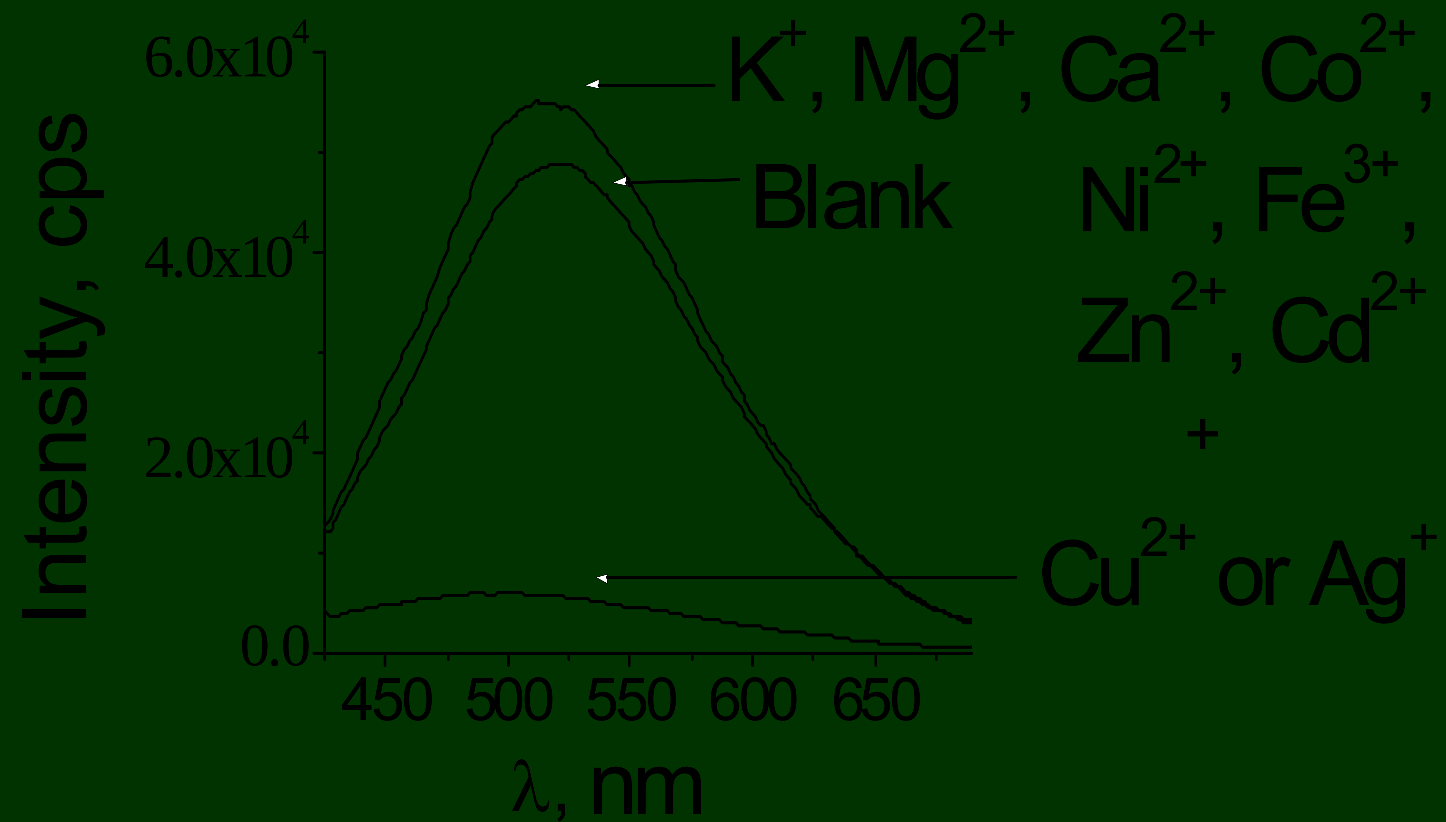

Differentiation = AgCl, insoluble & undetected

Gattás-Asfura, K. M. et al. Chem. Commun. 2003, 2684-2685.

CdS-Peptide QDs – Cu^{2+} Detection

Selectivity, comparison

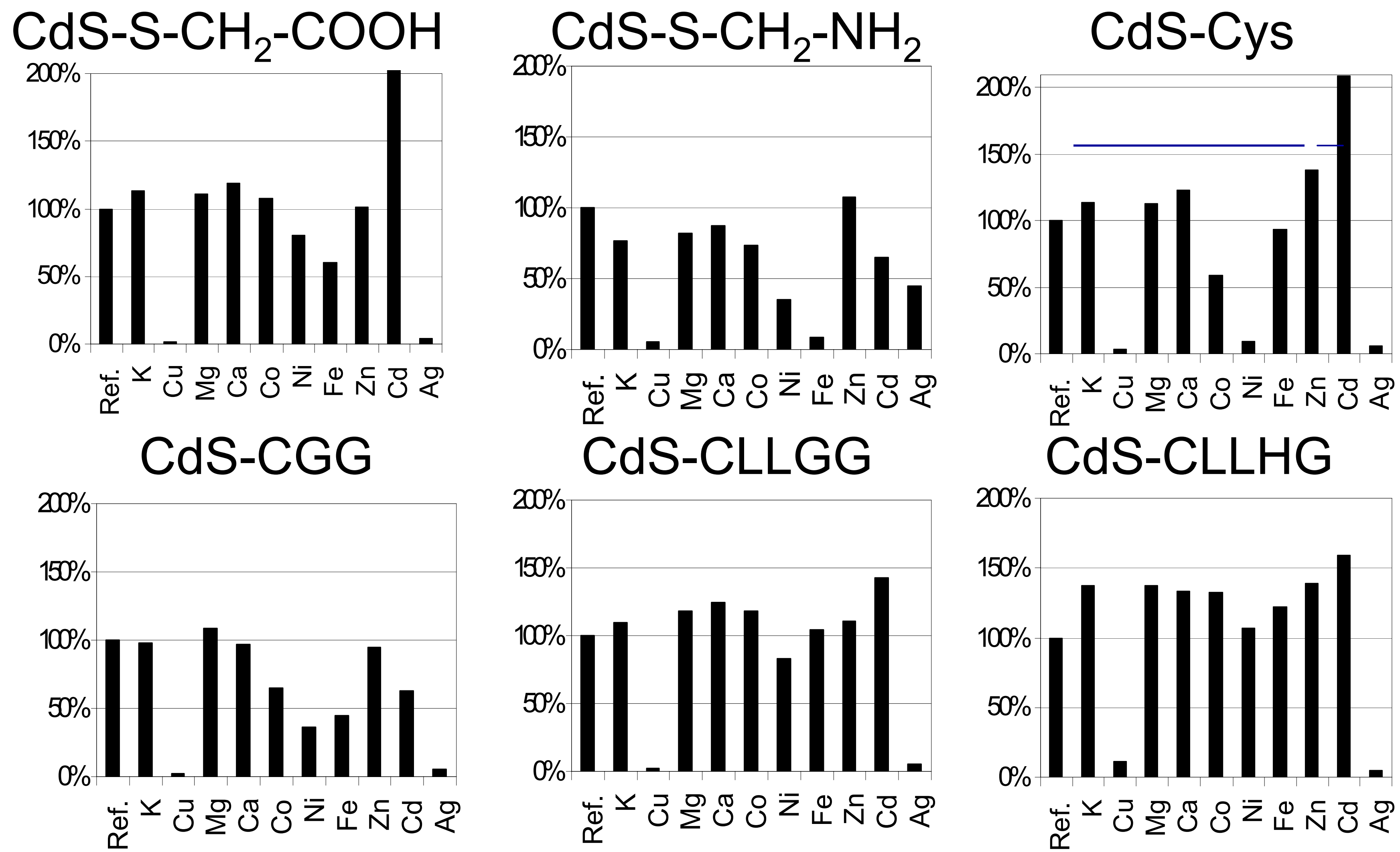

X = Metallic ions Y = Relative PL intensity

CdS-Peptide QDs – Cu^{2+} Detection

Detected Levels

- Max. PL quenching at a Cu^{2+}/QD molar ratio of 17:1 (ε_{QD} = 2 x 10^4 $M^{-1}cm^{-1}$)
- R^2 = 0.99 exponential fit (nM detection capability)

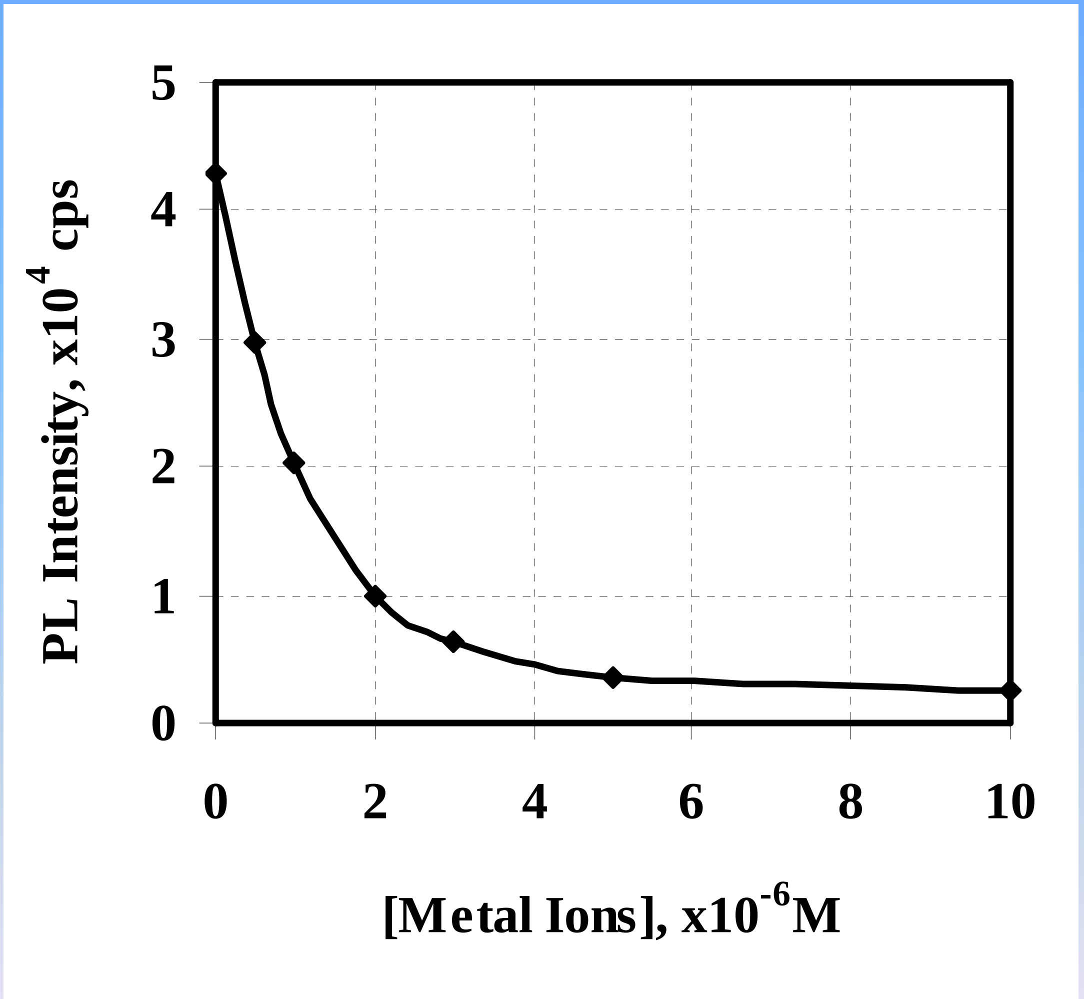

Gattás-Asfura, K. M. et al. Chem. Commun. 2003, 2684-2685.

Conclusions

- CdS-Cys-Leu-Leu-His-Gly QDs detected Cu^{2+} and Ag^{+} with high selectivity and sensitivity

- Leu-Leu and His-Gly residues played a critical role towards metallic ion selectivity

- Peptides facilitated fabrication of selective optical sensor by way of amino acid sequence design

Gattás-Asfura, K. M. et al. Chem. Commun. 2003, 2684-2685.

CdSe QDs Composite Film – Paraoxon Detection

✓ Layer-by-Layer technique (electrostatic interaction)

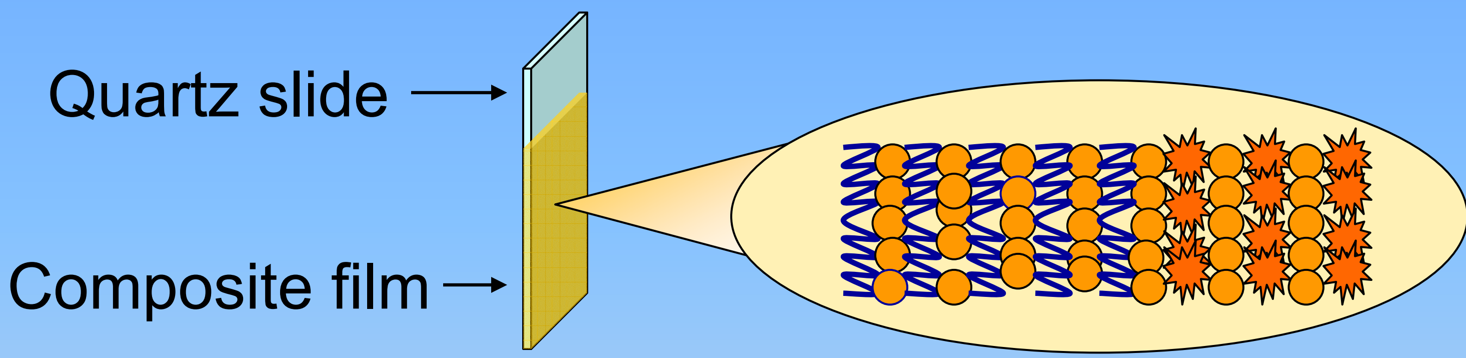

Chitosan

$CdSe\text{-}S\text{-}CH_2\text{-}COOH$ QDs

Organophosphorus hydrolase (OPH)

Constantine, C. A.; Gattas-Asfura, K. M.; Mello, S. V.; Crespo, G.; Rastogi, V.; Cheng, T.-C.; DeFrank, J. J.; Leblanc, R. M. *Langmuir;* **2003**; *19*(23); 9863-9867.

CdSe QDs Composite Film – Paraoxon Detection

Film growth

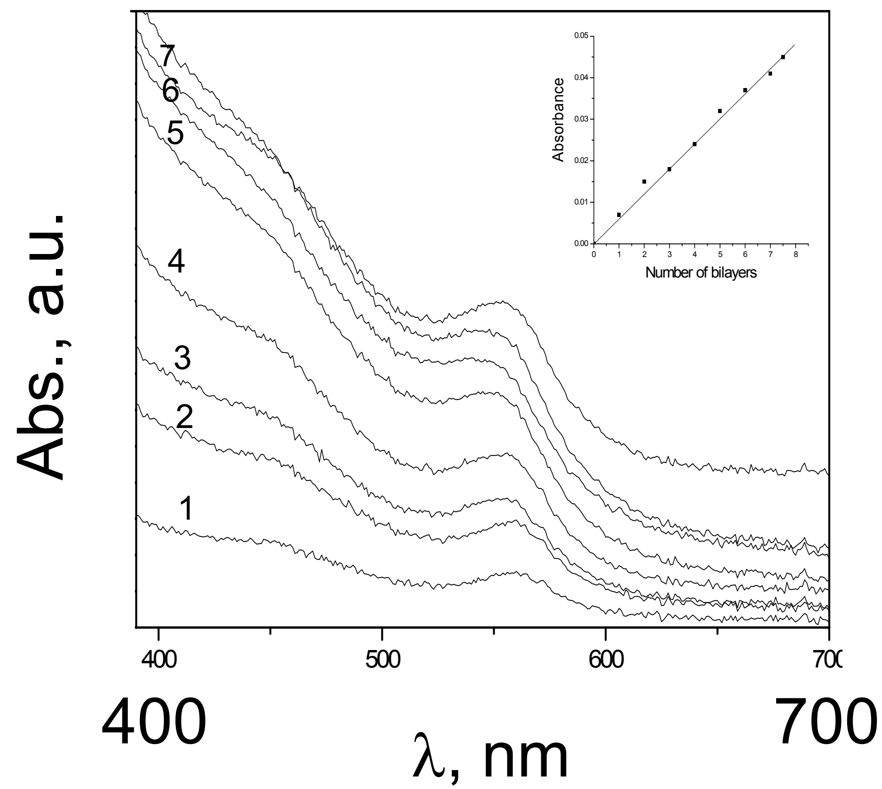

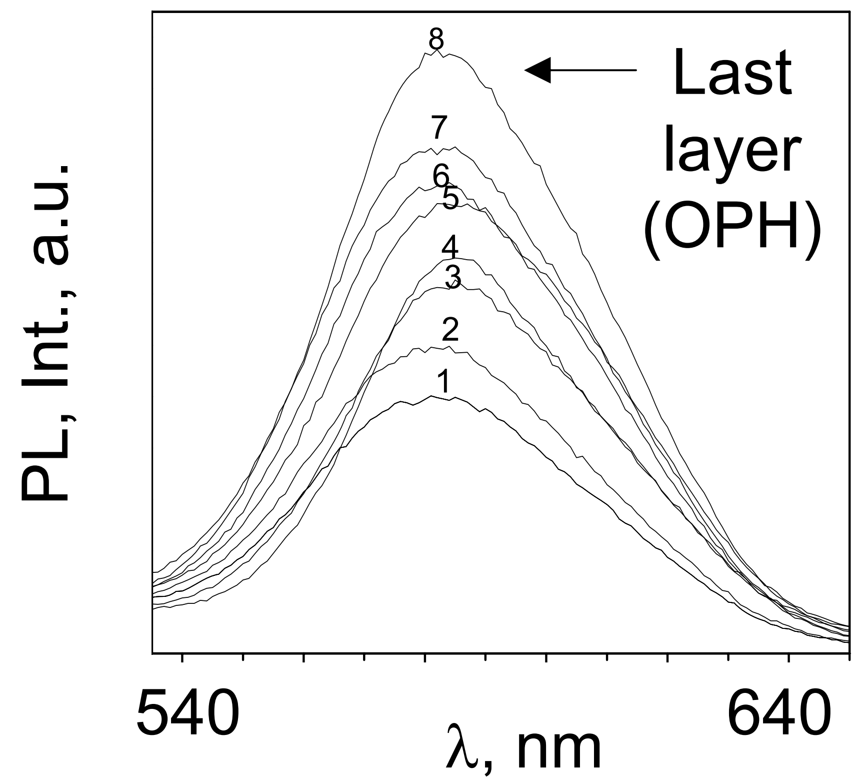

1-7 = # QDs layers

QD avg. size: 34 Å

Constantine, C. A.; Gattas-Asfura, K. M.; Mello, S. V.; Crespo, G.; Rastogi, V.; Cheng, T.-C.; DeFrank, J. J.; Leblanc, R. M. *Langmuir;* **2003**; *19*(23); 9863-9867.

CdSe QDs Composite Film – Paraoxon Detection

Response of film upon exposure to paraoxon

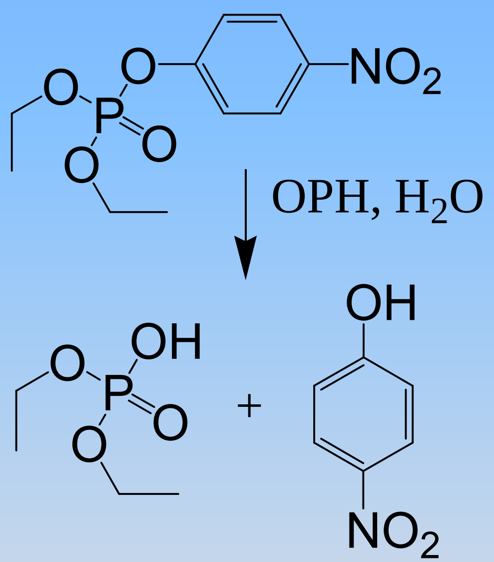

Paraoxon, 1×10^{-7} M

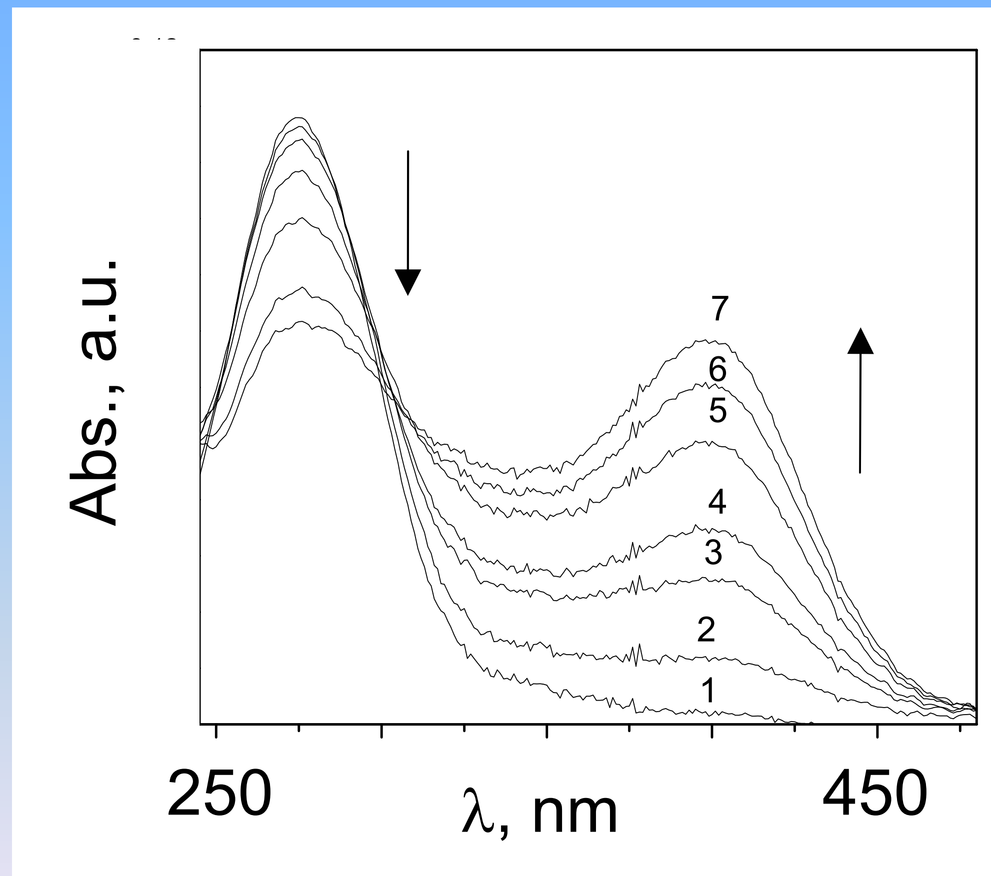

1-7 (bottom-top) = 0, 0.5, 1, 2, 5, 10, and 15 min.

Constantine, C. A.; Gattas-Asfura, K. M.; Mello, S. V.; Crespo, G.; Rastogi, V.; Cheng, T.-C.; DeFrank, J. J.; Leblanc, R. M. *Langmuir;* **2003**; *19*(23); 9863-9867.

CdSe QDs Composite Film – Paraoxon Detection

Response of film upon exposure to paraoxon

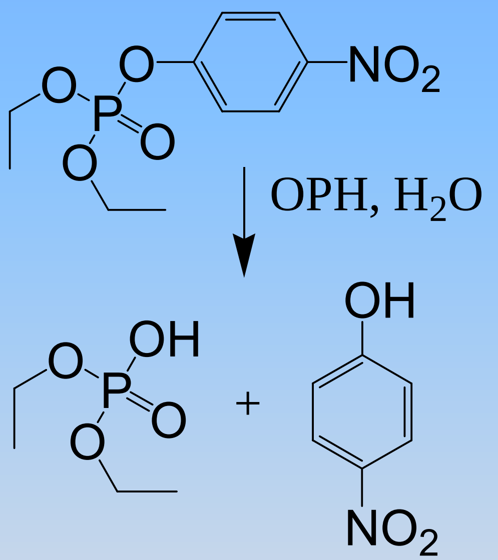

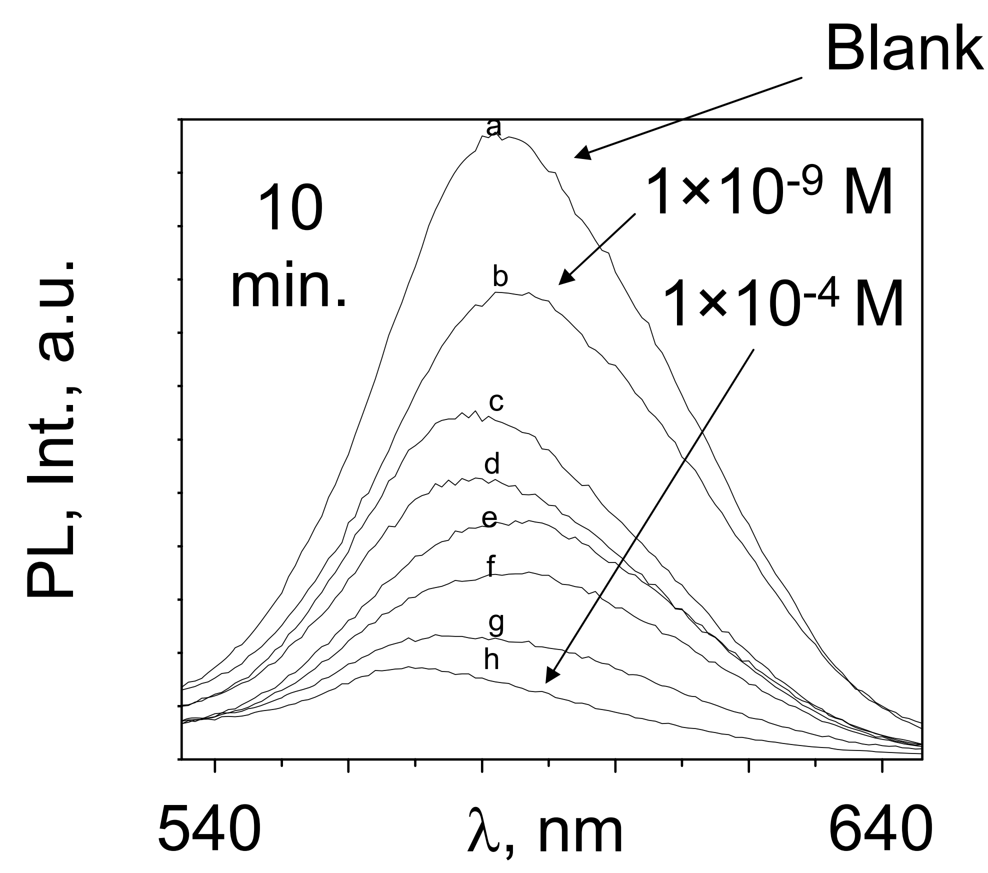

CdSe QDs Composite Film – Paraoxon Detection

Epifluorescence images of film

895μm × 793 μm

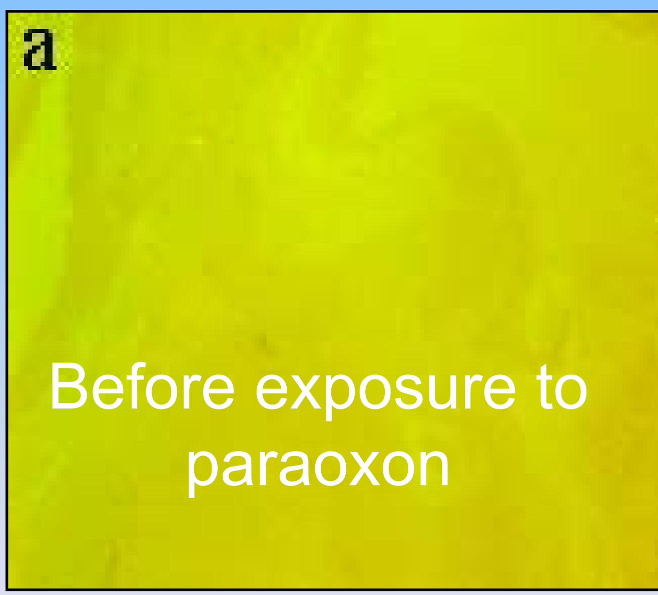

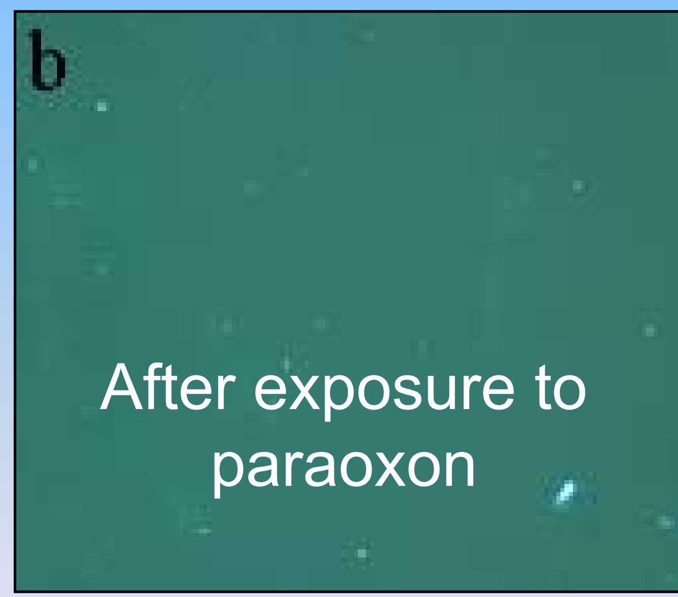

Conclusions

- QDs were successfully incorporated into composite films via the layer-by-layer technique and electrostatic interaction.
- The QDs/OPH ultra thin film selectively detected paraoxon at the nM levels.

Detection of paraoxon using QDs/OPH bioconjugate

Surface modification

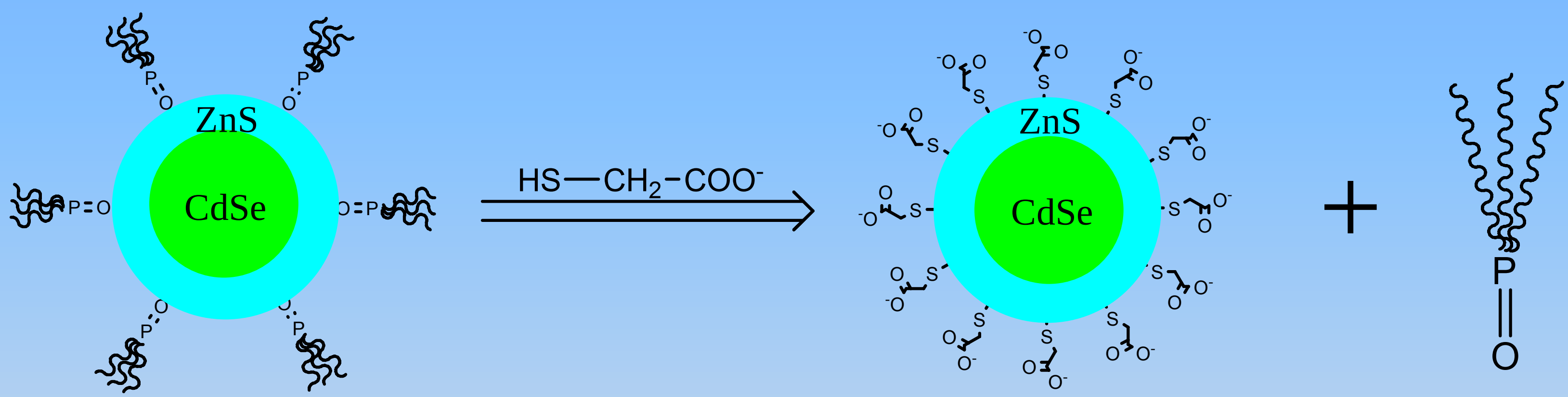

Hydrophobic

Hydrophilic

Ji, X. J.; Zheng, J.; Xu, J.; Rastogi, V. K.; Cheng, T. C.; DeFrank, J. J.; Leblanc R. M. *J. Phys. Chem. B* **2005**, *109*, 3793-3799.

Detection of paraoxon using QDs/OPH bioconjugate

Bioconjugation

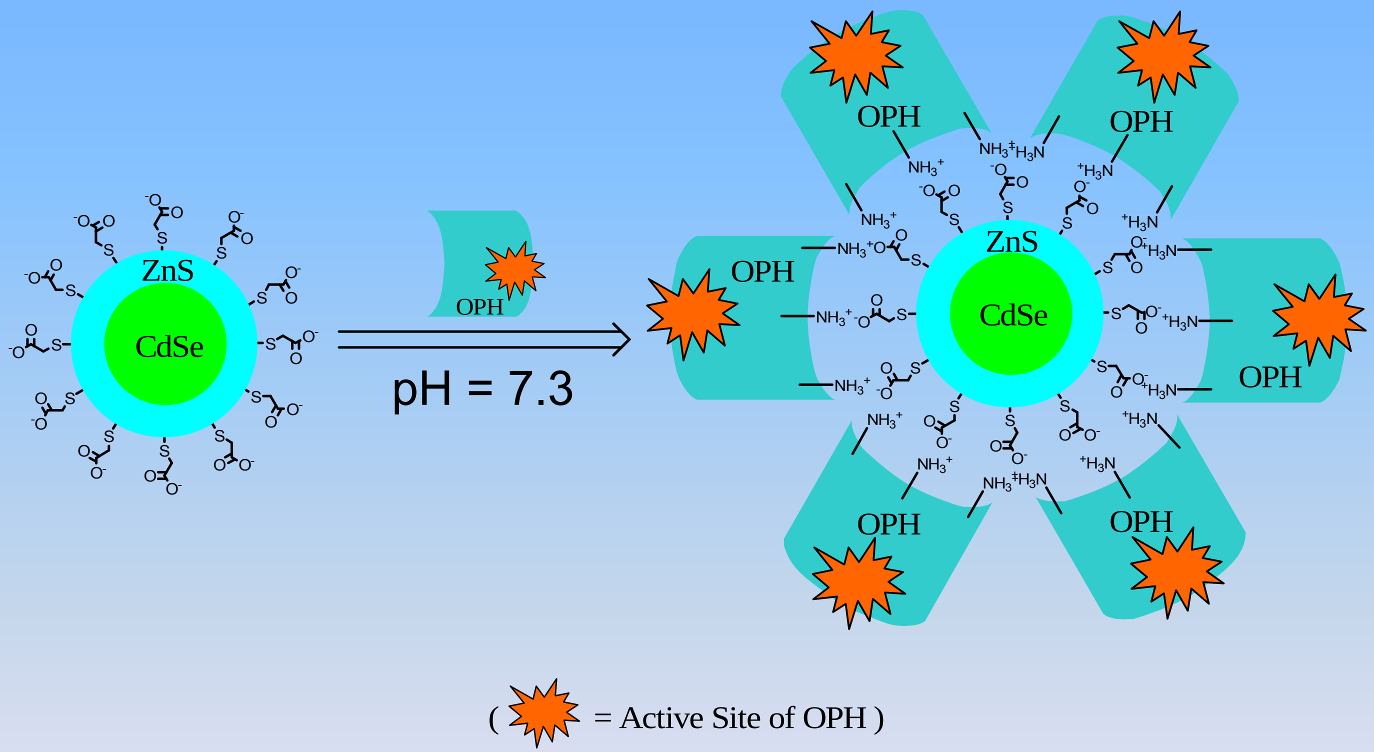

Isoelectric point of OPH : 7.6

Ji, X. J.; Zheng, J.; Xu, J.; Rastogi, V. K.; Cheng, T. C.; DeFrank, J. J.; Leblanc R. M. *J. Phys. Chem. B* **2005**, *109*, 3793-3799.

Detection of paraoxon using QDs/OPH bioconjugate

Secondary structure analysis of bioconjugates

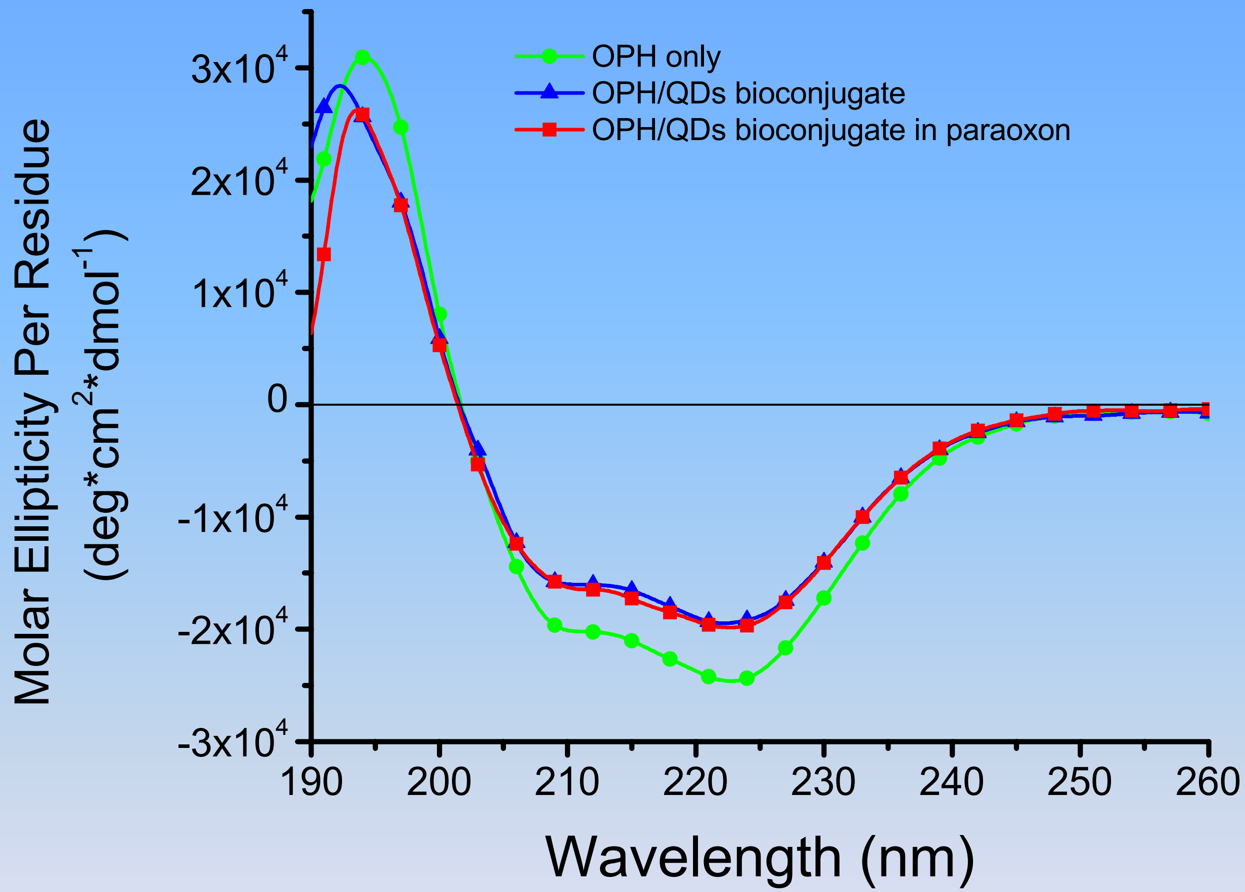

CD spectra of pure OPH and OPH/QDs bioconjugates with and without paraoxon. OPH concentration is 5×10^{-7} M in all cases. The OPH/QDs molar ratio of bioconjugates is 10. Paraoxon concentration is 10^{-6} M

Ji, X. J.; Zheng, J.; Xu, J.; Rastogi, V. K.; Cheng, T. C.; DeFrank, J. J.; Leblanc R. M. *J. Phys. Chem. B* **2005**, *109*, 3793-3799.

Detection of paraoxon using QDs/OPH bioconjugate

Secondary structure analysis of bioconjugates

	Percentage of Secondary Structure (%)					
	α-helix		β-strands		Turns (T)	Unordered (U)
	α_R	α_D	β_R	β_D		
OPH	40.03	25.53	2.40	4.43	13.67	15.53
OPH/QDs bioconjugates	36.10	21.43	3.37	4.10	13.10	20.07
OPH/QDs bioconjugates with paraoxon (10^{-6} M)	30.33	30.30	17.33	7.90	22.33	8.13

Secondary structure data of OPH, OPH/QDs bioconjugates and OPH/QDs bioconjugates in 10^{-6} M of paraoxon. The subscripts “R” and “D” represent “ordered” and “disordered”, respectively.

Ji, X. J.; Zheng, J.; Xu, J.; Rastogi, V. K.; Cheng, T. C.; DeFrank, J. J.; Leblanc R. M. *J. Phys. Chem. B* **2005**, *109*, 3793-3799.

Detection of paraoxon using QDs/OPH bioconjugate

Fluorescence responses of bioassay

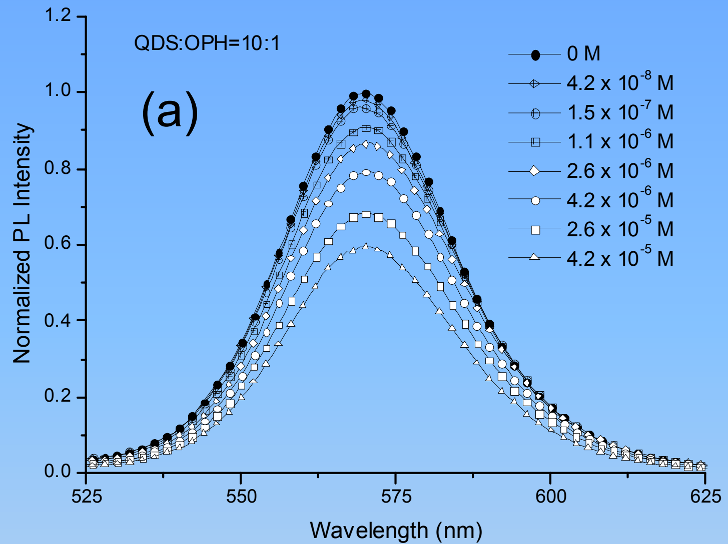

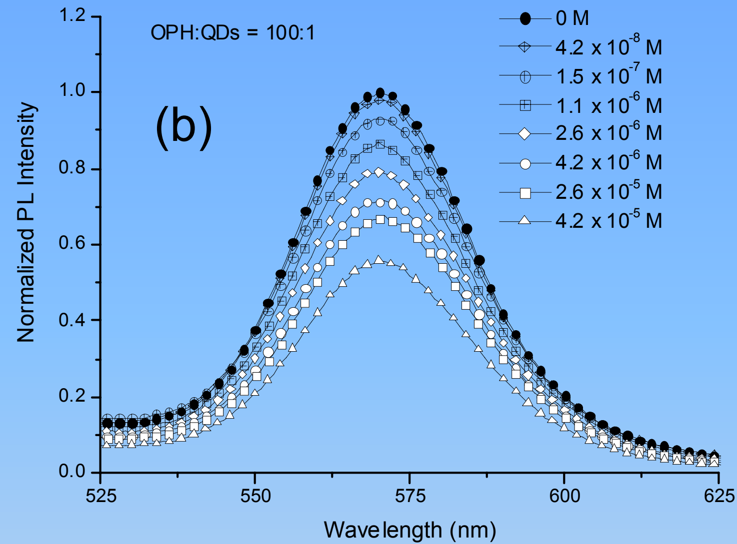

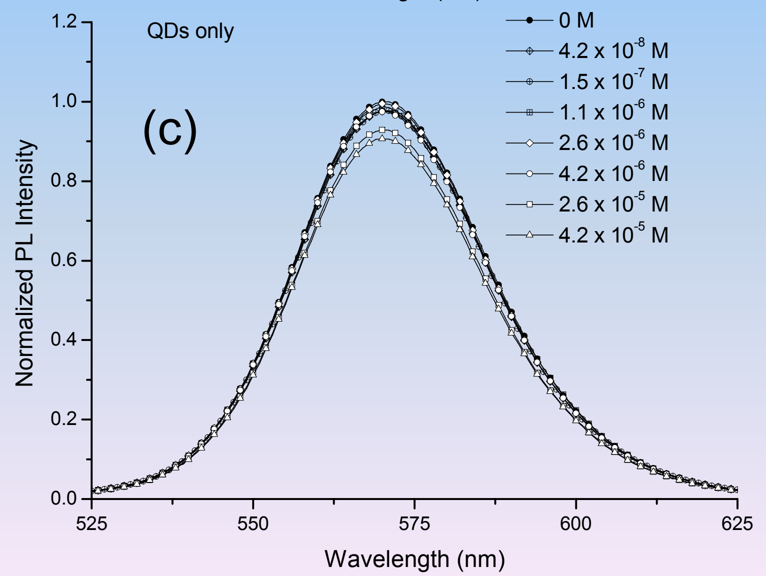

Photoluminescence spectra of **(a)** 10:1 and **(b)** 100:1 molar ratio OPH/QDs bioconjugates; **(c)** pure QDs in different concentrations of paraoxon. All samples were excited at 350 nm.

Ji, X. J.; Zheng, J.; Xu, J.; Rastogi, V. K.; Cheng, T. C.; DeFrank, J. J.; Leblanc R. M. *J. Phys. Chem. B* **2005**, *109*, 3793-3799.

Detection of paraoxon using QDs/OPH bioconjugate

Fluorescence responses of bioassay

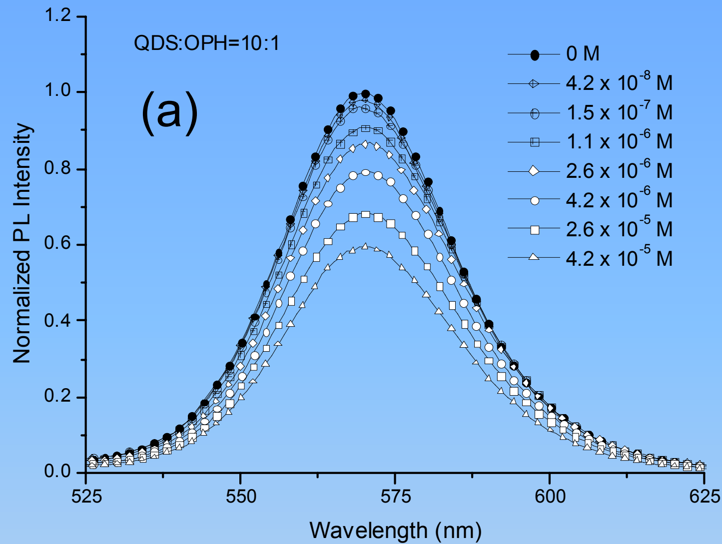

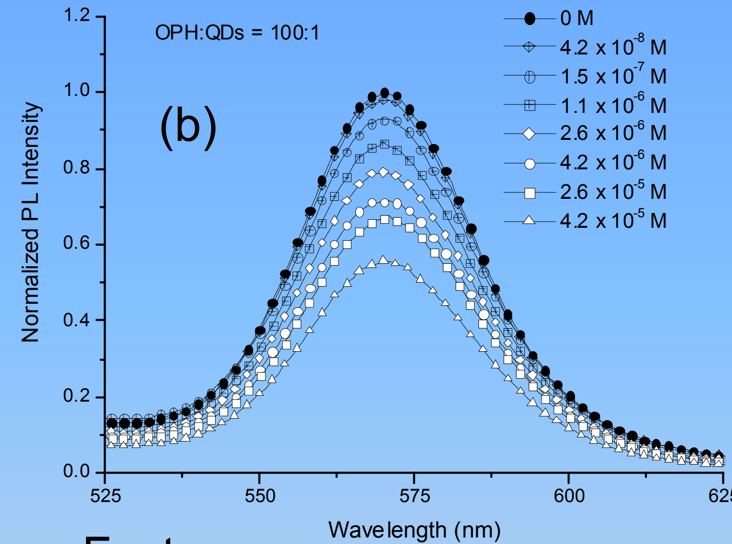

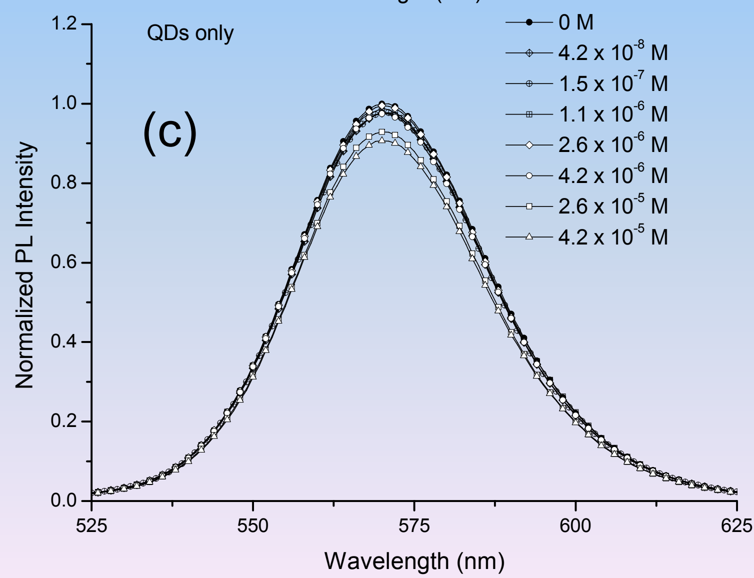

Facts:

1. The quenching of the PL is dependent to the concentration of paraoxon
2. The quenching of the PL has a maximum value in certain range of concentrations
3. The decrease of the PL intensity does not show a linear relationship to the [paraoxon]

Ji, X. J.; Zheng, J.; Xu, J.; Rastogi, V. K.; Cheng, T. C.; DeFrank, J. J.; Leblanc R. M. *J. Phys. Chem. B* **2005**, *109*, 3793-3799.

Detection of paraoxon using QDs/OPH bioconjugate

Proposed mechanism of quenching

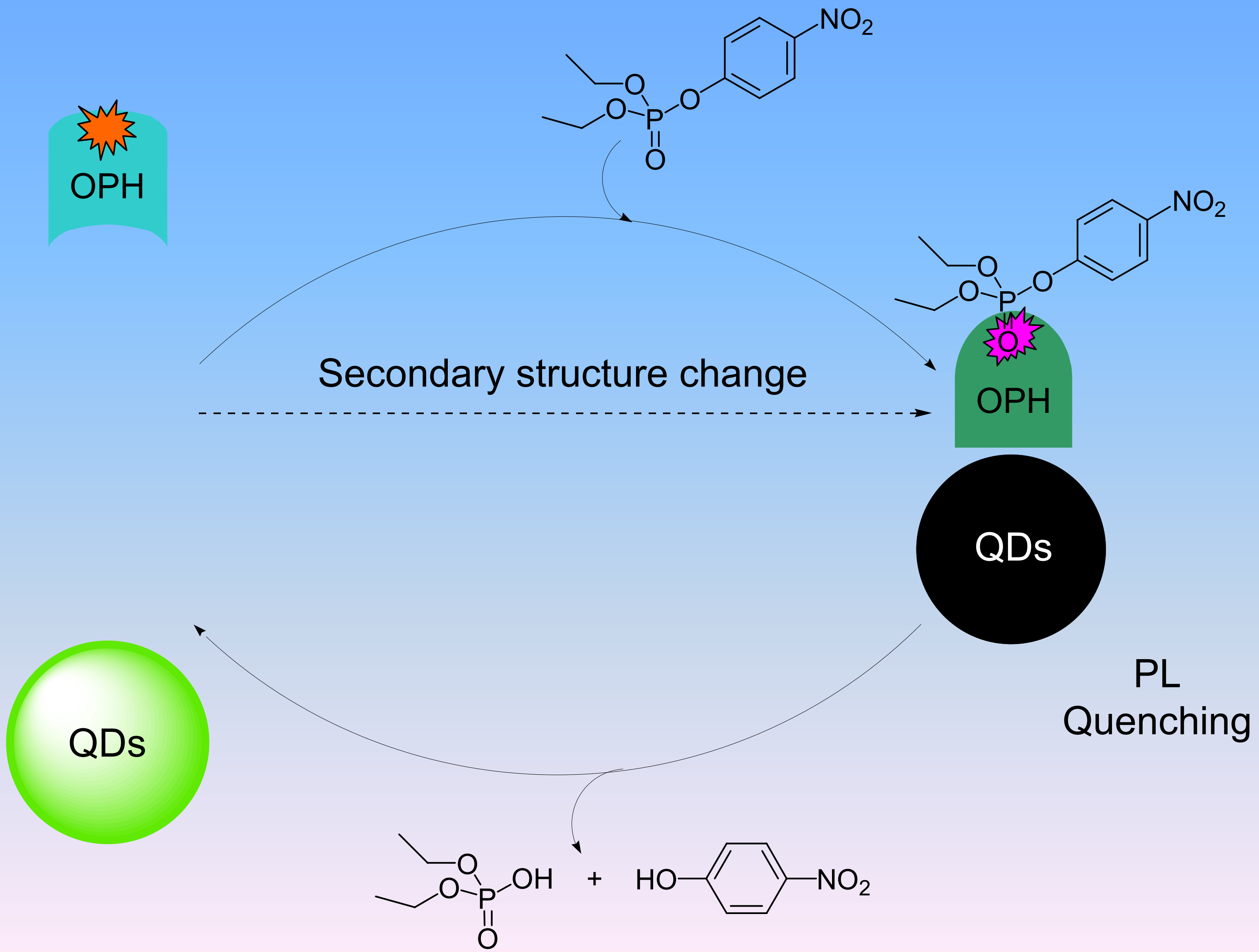

Detection of paraoxon using QDs/OPH bioconjugate

Effect of OPH:QDs molar ratio on the sensitivity of the bioassay

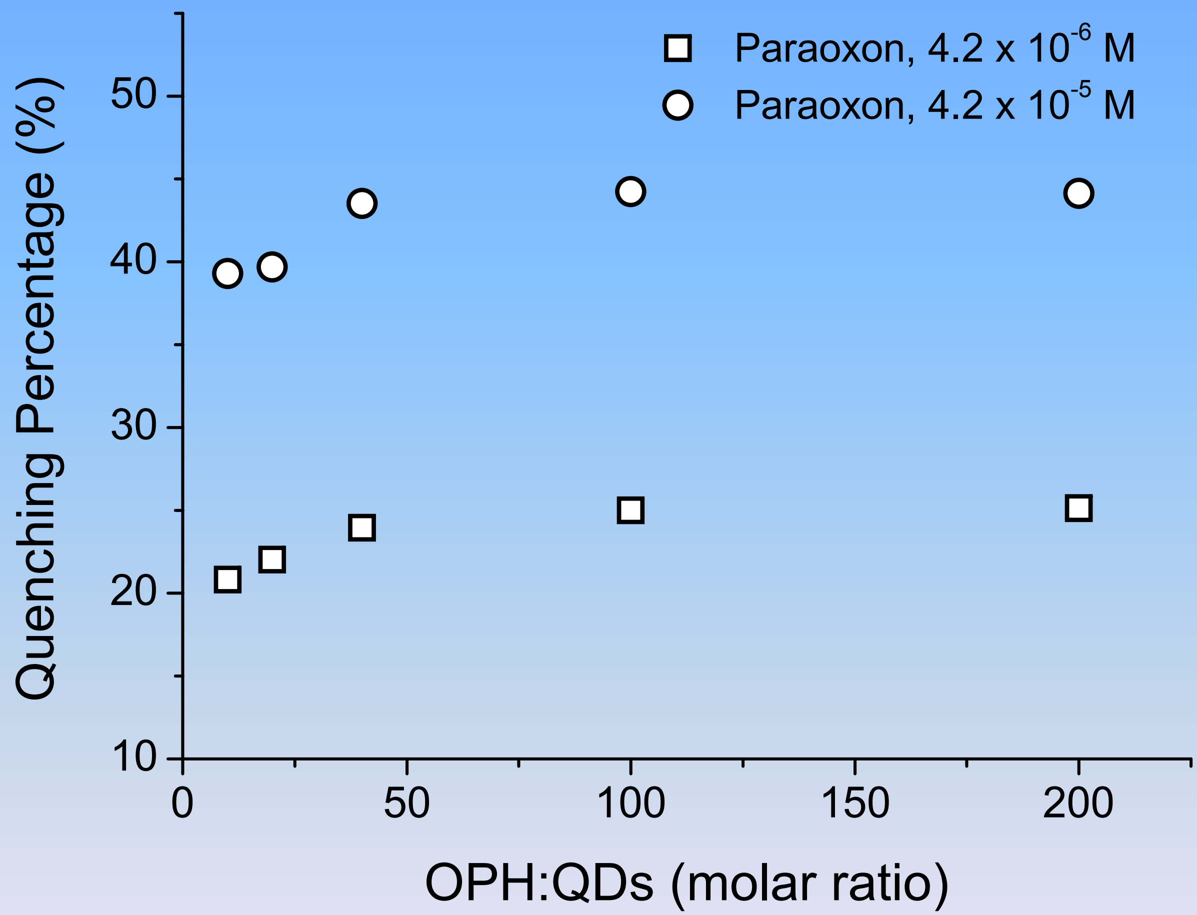

Concentration effect of OPH to the sensitivity of bioassay

Ji, X. J.; Zheng, J.; Xu, J.; Rastogi, V. K.; Cheng, T. C.; DeFrank, J. J.; Leblanc R. M. *J. Phys. Chem. B* **2005**, *109*, 3793-3799.

Conclusions

- The OPH and CdSe(ZnS) QDs can form stable bioconjugate through electrostatic interaction
- CD spectrum indicate a secondary structure change of OPH in presence of paraoxon
- The intensity of photoluminescence of OPH/QDs bioconjugate was quenched in presence of paraoxon
- The secondary structure change of OPH was responsible for the observed PL quenching
- Increasing the molar ratio of OPH over QDs will not increase the sensitivity of OPH/QDs biosensor

Imaging the formation of β-sheet using QDs/peptide conjugates

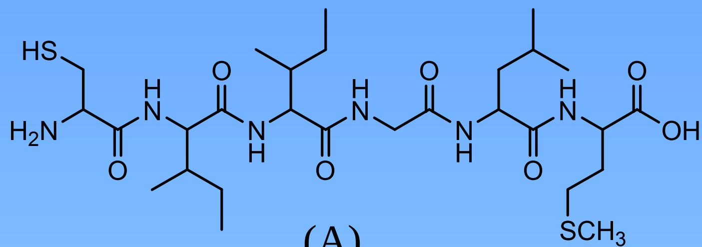

(A)

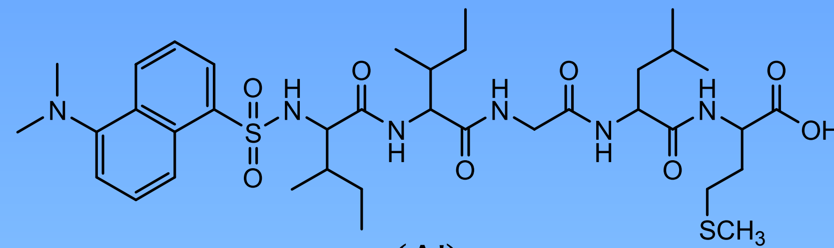

(A')

(B)

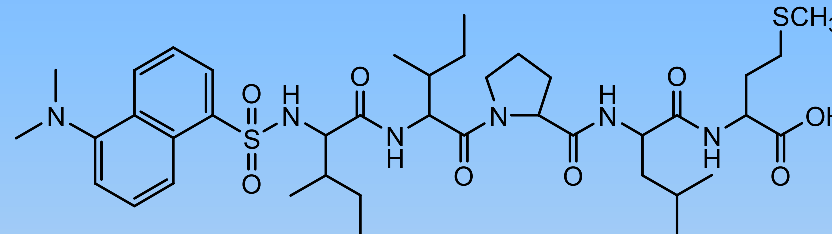

(B')

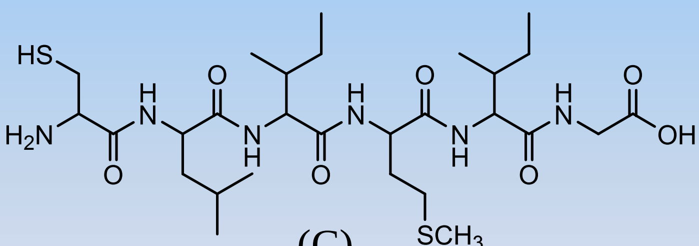

(C)

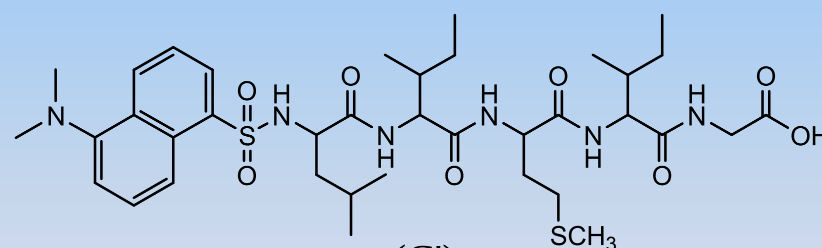

(C')

Structures of the synthetic peptides with cysteine linker and covalently bonded Dansyl group: (A) NH$_2$-Cys-Ile-Ile-Gly-Leu-Met-OH, (B) NH$_2$-Cys-Ile-Ile-Pro-Leu-Met-OH, (C) NH$_2$-Cys-Leu-Ile-Met-Ile-Gly-OH, (A') Dansyl-Ile-Ile-Gly-Leu-Met-OH, (B') Dansyl-Ile-Ile-Pro-Leu-Met-OH, and (C') Dansyl-Cys-Leu-Ile-Met-Ile-Gly-OH

Imaging the formation of β-sheet using QDs/peptide conjugates

Schematic illustration of the surface coating of synthetic peptide on TOPO-coated CdSe/ZnS

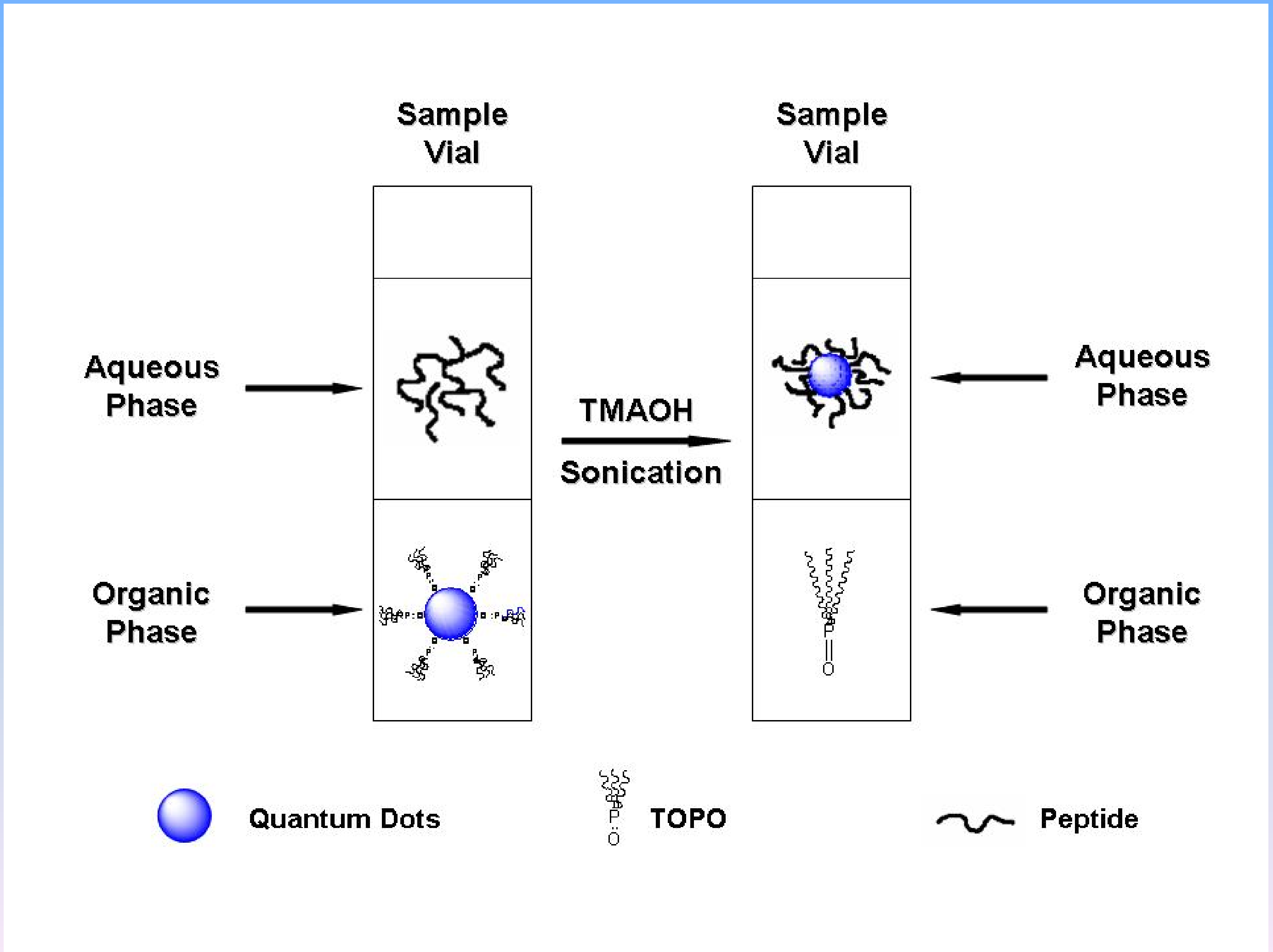

Imaging the formation of β-sheet using QDs/peptide conjugates

Steric configuration analysis by Circular Dichroism spectroscopy

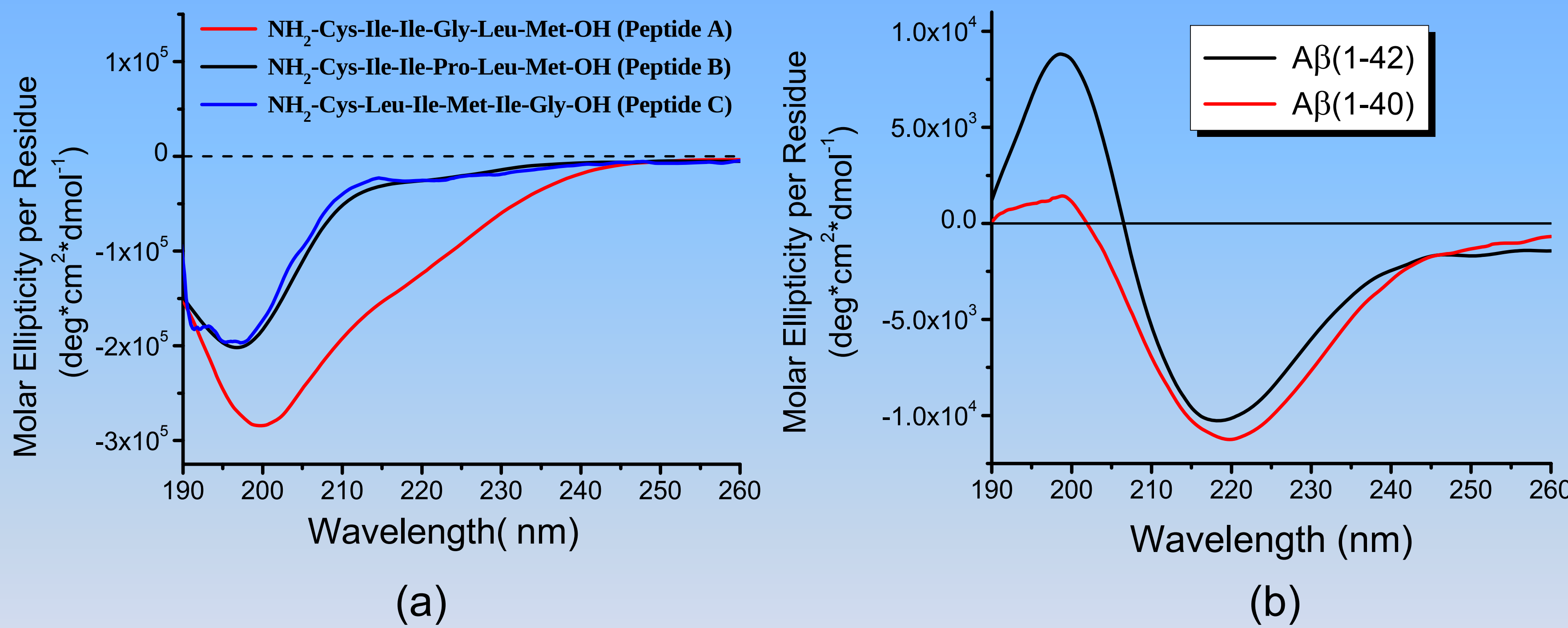

Circular Dichroism spectra of (a) three model peptides and (b) full length peptides.

Ji X., D,Naistat, C. Li, J. Orbulescu and R.M. Leblanc, Colloids and Surfaces B: Biointerfaces **2006**, in press.

Imaging the formation of β-sheet using QDs/peptide conjugates

Secondary structural data of Aβ (1-40), and Aβ (1-42) peptides. The subscripts "R" and "D" represent "ordered" and "disordered", respectively.

	Percentage of Secondary Structure					
	α-helix		β-strands		Turns (T)	Unordered (U)
	α_R	α_D	β_R	β_D		
Aβ (1-40)	12.5	11.3	18.5	8.5	19.0	30.2
Aβ (1-42)	11.8	9.5	22.6	14.5	14.0	27.5

Ji X., D,Naistat, C. Li, J. Orbulescu and R.M. Leblanc, Colloids and Surfaces B: Biointerfaces **2006**, in press.

Imaging the formation of β-sheet using QDs/peptide conjugates

Epifluorescence micrographs of 31-35 model peptides and controlled peptides

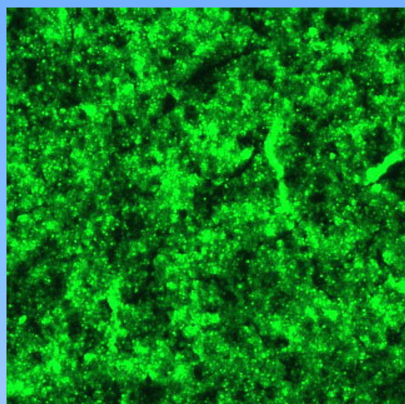

QDs-CIIGLM-OH

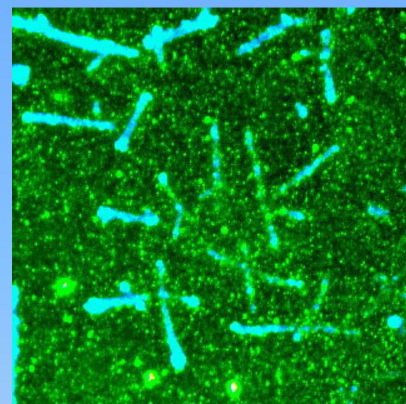

QDs-CIIPLM-OH

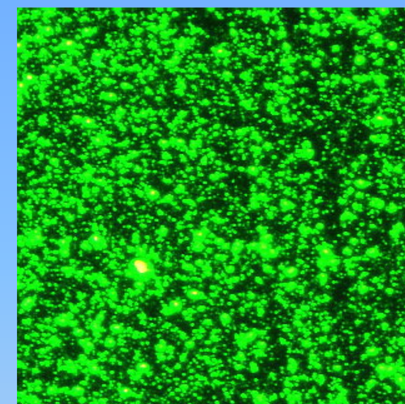

QDs-CLIMIG-OH

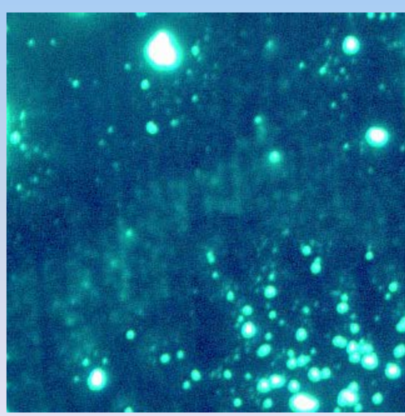

Dansyl-CIIGLM-OH

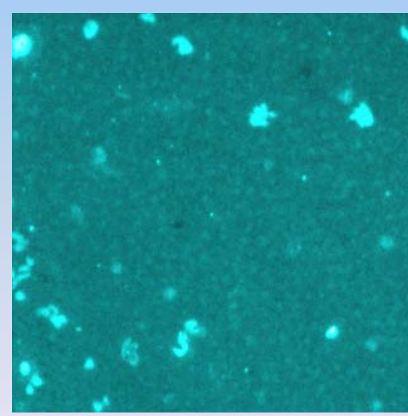

Dansyl-CIIPLM-OH

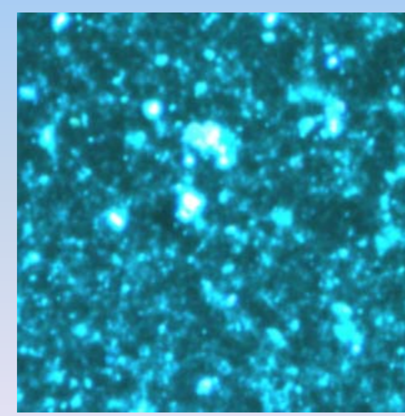

Dansyl-CLIMIG-OH

Ji X., D,Naistat, C. Li, J. Orbulescu and R.M. Leblanc, Colloids and Surfaces B: Biointerfaces **2006**, in press.

Imaging the formation of β-sheet using QDs/peptide conjugates

Epifluorescence micrographs of full length peptides

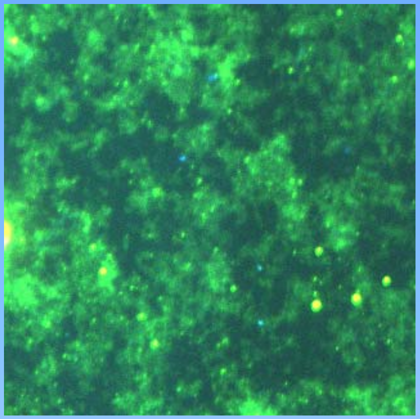

Aβ (1-40) / QDs mixture

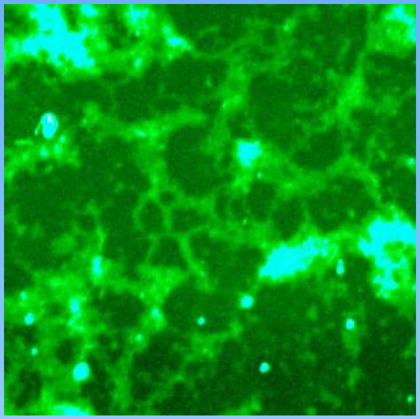

Aβ (1-42) / QDs mixture

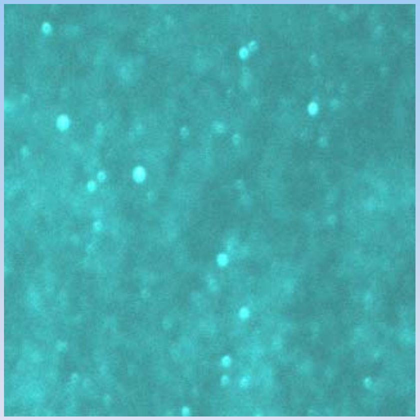

Aβ (1-40) / Dansyl acid mixture

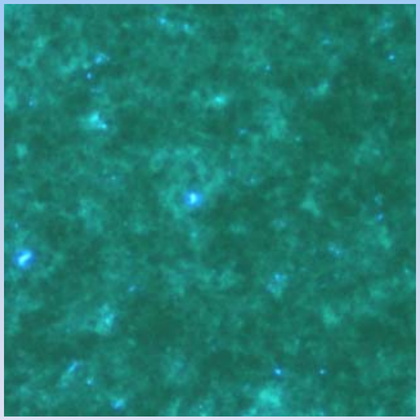

Aβ (1-42) / Dansyl acid mixture

Ji X., D,Naistat, C. Li, J. Orbulescu and R.M. Leblanc, Colloids and Surfaces B: Biointerfaces **2006**, in press.

Conclusions

- The model 31-35 Aβ peptides with cystein linker and Dansyl group were designed and synthesized
- A phase transfer approach was applied to conjugate the peptides onto the surface of the QDs
- The steric configuration study by CD spectroscopy revealed that the main secondary structural component of the aggregation is β-strands
- Epifluorescence microscopic research showed that QDs luminescent label approach showed a much higher intensity and better contrast for imaging than organic dye

Group Members

PhD Graduate Students:

- Jiayin Zheng (March 2006)
- Kerim M. Gattás-Asfura (December 2005)
- Xiaojun Ji (December 2005)
- David Naistat (December 2005)
- Changqing Li (June 2005)
- Robert Triulzi
- Jianmin Xu
- Liang Zhao

Sr. Research Associate:

- Jhony Orbulescu

Funding

National Science Foundation **U.S. Army Research Office**